

Performance Analysis of Mid-Infrared Quantum Cascade Lasers with Enhanced Optical Nonlinearity

Jing Bai and D. S. Citrin

*School of Electrical and Computer Engineering, Georgia Institute of Technology,
Atlanta, Georgia 30332-0250 USA*

Email: jbai@ece.gatech.edu, david.citrin@ece.gatech.edu

Abstract— We present simulations of mid-infrared quantum cascade lasers with optimized second-harmonic generation. The optimized design was obtained utilizing techniques from supersymmetric quantum mechanics with both material-dependent effective mass and band nonparabolicity. Two-photon processes are analyzed for the resonant cascading triple levels designed for enhancing second-harmonic generation. Nonunity pumping efficiency from one period of the QCL to the next is taken into account by including all relevant carrier scattering mechanisms between the injector/collector and active regions. Carrier transport and power output of the structure are analyzed by self-consistently solving rate equations for the carriers and photons. Current-dependent linear optical output power is derived based on the steady-state photon population in the active region. The second-harmonic (SH) power is derived from the Maxwell equations with the phase mismatch and modes overlapping included. Due to stronger coupling between lasing levels, the optimized structure has both higher linear and SH output powers. The optimized structure can be fabricated through digitally grading the submonolayer alloys by molecular beam epitaxy (MBE) technique.

I. INTRODUCTION

Nonlinearities in quantum cascade lasers (QCL's) can be greatly improved by tailoring the band profile, whereas increase the dipole matrix elements associated with intersubband transitions. In our previous work [1], we described the supersymmetric quantum mechanics optimization (SUSYQM) procedure [2] for the resonant second-order nonlinear susceptibility. In our present work, we continued to study the carrier transport and output performance of the optimized structure obtained in [1] with the inclusion of effects that can substantially impact the device performance, such as the nonunity pumping effect and phase-mismatching effect.

II. RATE-EQUATION MODEL OF OPTIMIZED STRUCTURE

We began with optimized structure obtained in our previous work [1]. The optimization is carried based on a published structure in Ref. [3], which is a lattice matched GaInAs/AlInAs QCL designed for second-harmonic

generation (SHG). The rate-equation model is built on the full cascade structure containing the injector, active region and collector, which is equal to 1.5 periods of the full cascade [4]. The active region, where laser emission and SHG take place, has five energy levels. Radiative transitions occur between the third and second states in the active region, denoted as 9 and 6. Levels 6, 9, 14, and 15 constitute two SHG cascades: 6-9-14 for cascade I and 9-14-15 for cascade II. The injector and collector contain five energy levels each. The curved profile of the optimized potential is obtained by modifying the mole fraction of the constituents of the ternary alloy system $\text{Ga}_x\text{In}_{1-x}\text{As}/\text{Al}_x\text{In}_{1-x}\text{As}$. In practice, the structure can be fabricated by digital-alloy growth [5]. The product of dipole matrix elements for cascade I increases by 60 % over the original value, while that for cascade II remains unchanged. The dipole matrix element between lasing levels increases by 35 %, which leads to larger oscillator strength between the lasing levels. The energy levels following optimization agree well with the ones for the original structure.

Due to the population redistribution amongst the levels, there will be competition between gain and the second-order nonlinear susceptibility, but the increased oscillator strength between lasing levels may alleviate the competition. In the 15-level rate equation model, the pumping loss from one period of the QCL to the next is taken into account by including all relevant electron-electron and electron-LO phonon scattering mechanisms between the injector/collector and active regions. In addition to the single-photon radiative transitions, our model also incorporates the sequentially and simultaneously resonant two-photon processes brought by the two SHG cascades. Unlike the single-photon transition rate, which is proportional to the incident photon density (light intensity), the two-photon stimulated emission/absorption rate is proportional to the squared photon density. The interplay between time-varying photon density in the cavity and radiative transition rates are all incorporated into our rate-equation model in order to investigate the lasing output.

We investigate the device performance for applied bias field between 30 kV/cm and 50 kV/cm, which is around the cascading bias 38 kV/cm. The steady-state solution is achieved through iteratively solving the rate equations to convergence.

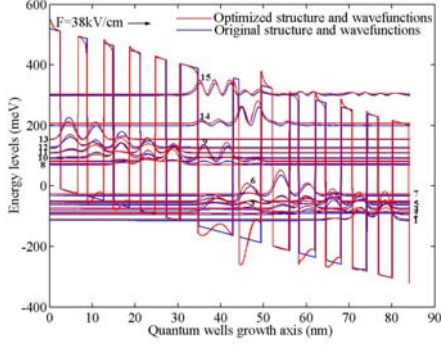


Fig. 1. Original and optimized band structures

III. RESULTS AND CONCLUSION

Our studies of the I-V characteristics of the original and optimized structures show that the current density in the optimized structure responds more sensitively to the applied bias due to enhanced NDR, as seen in Fig. 2. This can be attributed to the band-structure variation with the applied bias, which is completely decided by the geometry and material composition of the multiple quantum wells.

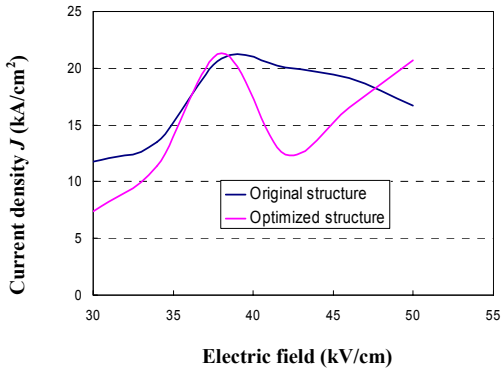


Fig. 2. I-V characteristic for the original and optimized structures.

The initial linear output intensity can be calculated from the steady-state photon densities in the cavity, while the SH power can be evaluated through the Maxwell's coupled wave equations including both phase-mismatching effect and modes overlap between fundamental and SH waves. Only TM modes are excited efficiently since the polarization associated with electronic intersubband transitions contains only the component along the crystal growth direction. According to the waveguide structure given in [3], the magnetic field intensity profile for TM modes at fundamental and SH frequencies are obtained as Fig. 3. In our following calculations, we pick up the TM_{00} modes at both frequencies since simulation results based on them are much closer to the experimental measurements reported in [3]. Figure 4 shows the linear and nonlinear output for both the original and optimized structure. The nonlinear power output is calculated under phase-mismatched condition. It can be seen that the threshold current is lowered in the optimized structure. The optimized structure has both higher linear and SH powers. With the SUSYQM optimized design, the linear-to-nonlinear conversion efficiency can achieve a two-fold enhancement over the original one.

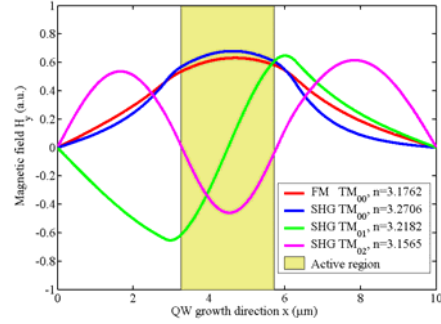


Fig. 3. Transverse magnetic field profiles for different modes

Our calculation shows that the nonlinear power output is only 10^{-4} of that under phase-matched conditions. Malis, *et al.* [6] reported that better phase matching are achieved between the TM_{00} fundamental mode and TM_{02} SHG mode, thus higher linear to nonlinear conversion efficiency greatly increased. However, that technique is a different physical concept as the SUSYQM optimization technique, which provides a means to improve the nonlinearity of the lasing medium.

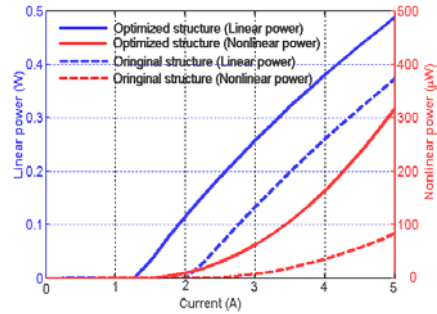


Fig. 4. Fundamental power and SH powers under different pump current for the original and optimized structures.

REFERENCES

- [1] J. Bai and D. S. Citrin, "Supersymmetric Optimization of Second-harmonic Generation in Mid-infrared Quantum Cascade Lasers," *Optics Express*, vol. 14, no. 9, pp. 4043-4048, 2006.
- [2] S. Tomić, V. Milanović and Z. Ikončić, "Optimization of intersubband resonant second-order susceptibility in asymmetric graded $Al_xGa_{1-x}As$ quantum wells using supersymmetric quantum mechanics," *Physical Review B*, vol. 56, no. 3, pp. 1033-1036, 1997.
- [3] G. Gmachl, A. Belyanin, D. L. Sivco, M. L. Peabody, N. Owschikow, A. M. Sergent, F. Capasso, and A. Y. Cho, "Optimized second-harmonic generation in quantum cascade lasers," *IEEE journal of Quantum electronics*, vol. 39, no. 11, pp. 1345-1355, Nov. 2003.
- [4] K. Donovan, P. Harrison, and R. W. Kelsall, "Self-consistent solutions to the intersubband rate equations in quantum cascade lasers: Analysis of a $GaAs/Al_xGa_{1-x}As$ device", *Journal of Applied Physics*, vol. 89, no. 6, 2001.
- [5] M. H. M. Reddy, A. Huntington, D. Duell, R. Koda, E. Hall, and L. A. Coldren, "Molecular-beam epitaxy growth of high-quality active regions with strained $In_xGa_{1-x}As$ quantum wells and lattice-matched $Al_xGa_{1-x}In_{1-x-y}As$ barriers using submonolayer superlattices," *Applied Physics Letters*, vol. 80, no. 19, pp.3509-3511, 2002.
- [6] O. Malis, *et al.*, "Improvement of second-harmonic generation in quantum-cascade lasers with true phase matching", *Applied Physics Letters*, vol. 84, no. 15, 2004.